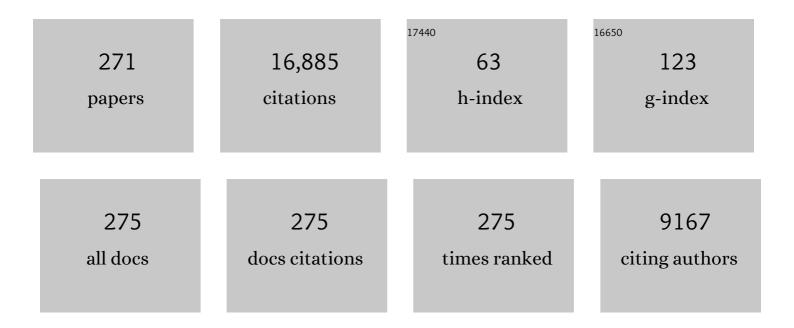
List of Publications by Year in descending order

Source: https://exaly.com/author-pdf/4955365/publications.pdf Version: 2024-02-01



#	Article	IF	CITATIONS
1	Diagnostic Performance in Low- and High-Contrast Tasks of an Image-Based Denoising Algorithm Applied to Radiation Dose–Reduced Multiphase Abdominal CT Examinations. American Journal of Roentgenology, 2023, 220, 73-85.	2.2	4
2	Improved visualization of the wrist at lower radiation dose with photon-counting-detector CT. Skeletal Radiology, 2023, 52, 23-29.	2.0	26
3	Comparison of glenohumeral joint kinematics between manual wheelchair tasks and implications on the subacromial space: A biplane fluoroscopy study. Journal of Electromyography and Kinesiology, 2022, 62, 102350.	1.7	8
4	Clinical evaluation of a phantom-based deep convolutional neural network for whole-body-low-dose and ultra-low-dose CT skeletal surveys. Skeletal Radiology, 2022, 51, 145-151.	2.0	11
5	Dual-Contrast Biphasic Liver Imaging With Iodine and Gadolinium Using Photon-Counting Detector Computed Tomography. Investigative Radiology, 2022, 57, 122-129.	6.2	25
6	Deepâ€learning model observer for a lowâ€contrast hepatic metastases localization task in computed tomography. Medical Physics, 2022, 49, 70-83.	3.0	7
7	Simultaneous dualâ€contrast imaging using energyâ€integrating detector multiâ€energy CT: An in vivo feasibility study. Medical Physics, 2022, 49, 1458-1467.	3.0	3
8	Dependence of Water-equivalent Diameter and Size-specific Dose Estimates on CT Tube Potential. Radiology, 2022, 303, 404-411.	7.3	4
9	First Clinical Photon-counting Detector CT System: Technical Evaluation. Radiology, 2022, 303, 130-138.	7.3	201
10	A New Frontier in Temporal Bone Imaging: Photon-Counting Detector CT Demonstrates Superior Visualization of Critical Anatomic Structures at Reduced Radiation Dose. American Journal of Neuroradiology, 2022, 43, 579-584.	2.4	43
11	Technical note: Evaluation of Artificial 120â€kilovolt computed tomography images for radiation therapy applications. Medical Physics, 2022, , .	3.0	1
12	Improved assessment of coronary artery luminal stenosis with heavy calcifications using high-resolution photon-counting detector CT. , 2022, , .		9
13	Impact of improved spatial resolution on radiomic features using photon-counting-detector CT. , 2022, , $\cdot$		4
14	A 25-reader performance study for hepatic metastasis detection: lessons from unsupervised learning. , 2022, , .		1
15	Improving coronary artery imaging in single source CT with cardiac motion correction using attention and spatial transformer based neural networks. , 2022, , .		2
16	Quantification of coronary calcification using high-resolution photon-counting-detector CT and an image domain denoising algorithm. , 2022, , .		5
17	Quantitative assessment of motion effects in dual-source dual energy CT and dual-source photon-counting detector CT. , 2022, , .		1
18	Utility of an automatic adaptive iterative metal artifact reduction AiMAR algorithm in improving CT imaging of patients with hip prostheses evaluated for suspected bladder malignancy. Abdominal Radiology, 2022, 47, 2158-2167.	2.1	3

#	Article	IF	CITATIONS
19	Estimating the Clinical Impact of Photon-Counting-Detector CT in Diagnosing Usual Interstitial Pneumonia. Investigative Radiology, 2022, 57, 734-741.	6.2	34
20	Ultra-high-resolution imaging of the shoulder and pelvis using photon-counting-detector CT: a feasibility study in patients. European Radiology, 2022, 32, 7079-7086.	4.5	31
21	A minimum SNR criterion for computed tomography object detection in the projection domain. Medical Physics, 2022, 49, 4988-4998.	3.0	5
22	Clinical evaluation of a new adaptive iterative metal artifact reduction method in whole-body low-dose CT skeletal survey examinations. Skeletal Radiology, 2021, 50, 149-157.	2.0	2
23	Benefits of iterative metal artifact reduction and dual-energy CT towards mitigating artifact in the setting of total shoulder prostheses. Skeletal Radiology, 2021, 50, 51-58.	2.0	10
24	Lowâ€dose CT image and projection dataset. Medical Physics, 2021, 48, 902-911.	3.0	89
25	X-Ray Transmittance Modeling-Based Material Decomposition Using a Photon-Counting Detector CT System. IEEE Transactions on Radiation and Plasma Medical Sciences, 2021, 5, 508-516.	3.7	5
26	Photon Counting CT: Clinical Applications and Future Developments. IEEE Transactions on Radiation and Plasma Medical Sciences, 2021, 5, 441-452.	3.7	68
27	Technical Note: kVâ€independent coronary calcium scoring: A phantom evaluation of score accuracy and potential radiation dose reduction. Medical Physics, 2021, 48, 1307-1314.	3.0	10
28	The feasibility of low iodine dynamic CT angiography with test bolus for evaluation of lower extremity peripheral artery disease. Vascular, 2021, 29, 170853812098630.	0.9	0
29	Empirical beam hardening and ring artifact correction for xâ€ray grating interferometry (EBHCâ€GI). Medical Physics, 2021, 48, 1327-1340.	3.0	0
30	High resolution, full field of view, whole body photon-counting detector CT: system assessment and initial experience. , 2021, 11595, .		5
31	A web-based software platform for efficient and quantitative CT image quality assessment and protocol optimization. , 2021, 11595, .		2
32	Random search as a neural network optimization strategy for Convolutional-Neural-Network (CNN)-based noise reduction in CT. , 2021, 11596, .		10
33	Deep-learning lesion and noise insertion for virtual clinical trial in chest CT. , 2021, 11595, .		0
34	Basal Ganglia Calcification Is Associated With Local and Systemic Metabolic Mechanisms in Adult Hypoparathyroidism. Journal of Clinical Endocrinology and Metabolism, 2021, 106, 1900-1917.	3.6	7
35	Improved coronary calcification quantification using photon-counting-detector CT: an ex vivo study in cadaveric specimens. European Radiology, 2021, 31, 6621-6630.	4.5	37
36	Automated radiomic analysis of CT images to predict likelihood of spontaneous passage of symptomatic renal stones. Emergency Radiology, 2021, 28, 781-788.	1.8	6

#	Article	IF	CITATIONS
37	Deep-learning-based direct synthesis of low-energy virtual monoenergetic images with multi-energy CT. Journal of Medical Imaging, 2021, 8, 052104.	1.5	8
38	Implementation and experimental evaluation of Mega-voltage fan-beam CT using a linear accelerator. Radiation Oncology, 2021, 16, 139.	2.7	1
39	The utility of a dual-phase, dual-energy CT protocol in patients presenting with overt gastrointestinal bleeding. Acta Radiologica Open, 2021, 10, 205846012110306.	0.6	3
40	Full field-of-view, high-resolution, photon-counting detector CT: technical assessment and initial patient experience. Physics in Medicine and Biology, 2021, 66, 205019.	3.0	54
41	Evaluating a Convolutional Neural Network Noise Reduction Method When Applied to CT Images Reconstructed Differently Than Training Data. Journal of Computer Assisted Tomography, 2021, 45, 544-551.	0.9	17
42	Energyâ€integratingâ€detector multiâ€energy CT: Implementation and a phantom study. Medical Physics, 2021, 48, 4857-4871.	3.0	2
43	Deep learning enabled ultraâ€fastâ€pitch acquisition in clinical Xâ€ray computed tomography. Medical Physics, 2021, 48, 5712-5726.	3.0	5
44	Reader Performance as a Function of Patient Size for the Detection of Hepatic Metastases. Journal of Computer Assisted Tomography, 2021, Publish Ahead of Print, 812-819.	0.9	0
45	Computed tomography turns 50. Physics Today, 2021, 74, 34-40.	0.3	12
46	CT Noise-Reduction Methods for Lower-Dose Scanning: Strengths and Weaknesses of Iterative Reconstruction Algorithms and New Techniques. Radiographics, 2021, 41, 1493-1508.	3.3	41
47	An interactive eyeâ€ŧracking system for measuring radiologists' visual fixations in volumetric CT images: Implementation and initial eyeâ€ŧracking accuracy validation. Medical Physics, 2021, 48, 6710-6723.	3.0	4
48	A Pilot Study to Estimate the Impact of High Matrix Image Reconstruction on Chest Computed Tomography. Journal of Clinical Imaging Science, 2021, 11, 52.	1.1	4
49	Procedure for optimal implementation of automatic tube potential selection in pediatric CT to reduce radiation dose and improve workflow. Journal of Applied Clinical Medical Physics, 2021, 22, 194-202.	1.9	1
50	Evaluation of Pseudoreader Study Designs to Estimate Observer Performance Results as an Alternative to Fully Crossed, Multireader, Multicase Studies. Academic Radiology, 2020, 27, 244-252.	2.5	1
51	Synthesizing images from multiple kernels using a deep convolutional neural network. Medical Physics, 2020, 47, 422-430.	3.0	26
52	Prior iterative reconstruction (PIR) to lower radiation dose and preserve radiologist performance for multiphase liver CT: a multi-reader pilot study. Abdominal Radiology, 2020, 45, 45-54.	2.1	5
53	Quantitative accuracy and dose efficiency of dualâ€contrast imaging using dualâ€energy CT: a phantom study. Medical Physics, 2020, 47, 441-456.	3.0	13
54	Dose Reduction for Sinus and Temporal Bone Imaging Using Photon-Counting Detector CT With an Additional Tin Filter. Investigative Radiology, 2020, 55, 91-100.	6.2	86

#	Article	IF	CITATIONS
55	Electrocardiogram-Gated Computed Tomography with Coronary Angiography for Cardiac Substructure Delineation and Sparing in Patients with Mediastinal Lymphomas Treated with Radiation Therapy. Practical Radiation Oncology, 2020, 10, 104-111.	2.1	8
56	Shoulder mechanical impingement risk associated with manual wheelchair tasks in individuals with spinal cord injury. Clinical Biomechanics, 2020, 71, 221-229.	1.2	18
57	Observer Performance for Detection of Pulmonary Nodules at Chest CT over a Large Range of Radiation Dose Levels. Radiology, 2020, 297, 699-707.	7.3	15
58	Deepâ€learningâ€based direct inversion for material decomposition. Medical Physics, 2020, 47, 6294-6309.	3.0	26
59	Fat quantification of the rotator cuff musculature using dual-energy CT–A pilot study. European Journal of Radiology, 2020, 130, 109145.	2.6	11
60	Wave optics simulation of gratingâ€based Xâ€ray phaseâ€contrast imaging using 4D Mouse Whole Body (MOBY) phantom. Medical Physics, 2020, 47, 5761-5771.	3.0	3
61	Quantitative Knee Arthrography in a Large Animal Model of Osteoarthritis Using Photon-Counting Detector CT. Investigative Radiology, 2020, 55, 349-356.	6.2	22
62	Multi-energy CT imaging for large patients using dual-source photon-counting detector CT. Physics in Medicine and Biology, 2020, 65, 17NT01.	3.0	14
63	The evolving role of imaging for small bowel neuroendocrine neoplasms: estimated impact of imaging and disease-free survival in a retrospective observational study. Abdominal Radiology, 2020, 45, 623-631.	2.1	10
64	lmage quality in abdominal CT using an iodine contrast reduction algorithm employing patient size and weight and low kV CT technique. Acta Radiologica, 2020, 61, 1186-1195.	1.1	4
65	A Universal Protocol for Abdominal CT Examinations Performed on a Photon-Counting Detector CT System. Investigative Radiology, 2020, 55, 226-232.	6.2	24
66	Noise reduction in CT image using prior knowledge aware iterative denoising. Physics in Medicine and Biology, 2020, , .	3.0	6
67	Deep-learning-based model observer for a lung nodule detection task in computed tomography. Journal of Medical Imaging, 2020, 7, 1.	1.5	9
68	Reducing Heart Dose with Protons and Cardiac Substructure Sparing for Mediastinal Lymphoma Treatment. International Journal of Particle Therapy, 2020, 7, 1-12.	1.8	8
69	A Blooming correction technique for improved vasa vasorum detection using an ultra-high-resolution photon-counting detector CT. , 2020, 11312, .		3
70	Multi-energy CT with triple X-ray beams: a feasibility animal study. , 2020, 11312, .		0
71	Overcoming calcium blooming and improving the quantification accuracy of percent area luminal stenosis by material decomposition of multi-energy computed tomography datasets. Journal of Medical Imaging, 2020, 7, 053501.	1.5	5
72	Technical Note: Increased photon starvation artifacts at low helical pitch in ultraâ€lowâ€dose CT. Medical Physics, 2019, 46, 5538-5543.	3.0	1

#	Article	IF	CITATIONS
73	Radiation dose efficiency of multi-energy photon-counting-detector CT for dual-contrast imaging. Physics in Medicine and Biology, 2019, 64, 245003.	3.0	22
74	State of the Art in Abdominal CT: The Limits of Iterative Reconstruction Algorithms. Radiology, 2019, 293, 491-503.	7.3	126
75	Reducing radiation dose for multi-phase contrast-enhanced dual energy renal CT: pilot study evaluating prior iterative reconstruction. Abdominal Radiology, 2019, 44, 3350-3358.	2.1	4
76	Computed Tomography Technology—and Dose—in the 21st Century. Health Physics, 2019, 116, 157-162.	0.5	17
77	Renal Adiposity Does not Preclude Quantitative Assessment of Renal Function Using Dual-Energy Multidetector CT in Mildly Obese Human Subjects. Academic Radiology, 2019, 26, 1488-1494.	2.5	6
78	Feasibility of multiâ€contrast imaging on dualâ€source photon counting detector (PCD) CT: An initial phantom study. Medical Physics, 2019, 46, 4105-4115.	3.0	41
79	Clinical utility of virtual noncalcium dual-energy CT in imaging of the pelvis and hip. Skeletal Radiology, 2019, 48, 1833-1842.	2.0	6
80	Symptomatic and Radiographic Manifestations of Kidney Stone Recurrence and Their Prediction by Risk Factors: A Prospective Cohort Study. Journal of the American Society of Nephrology: JASN, 2019, 30, 1251-1260.	6.1	48
81	Dual-Energy CT Monitoring of Cryoablation Zone Growth in the Spinal Column and Bony Pelvis: A Laboratory Study. Journal of Vascular and Interventional Radiology, 2019, 30, 1496-1503.	0.5	9
82	Photon-counting Detector CT: System Design and Clinical Applications of an Emerging Technology. Radiographics, 2019, 39, 729-743.	3.3	270
83	Localization of liver lesions in abdominal CT imaging: I. Correlation of human observer performance between anatomical and uniform backgrounds. Physics in Medicine and Biology, 2019, 64, 105011.	3.0	9
84	Dual-source photon counting detector CT with a tin filter: a phantom study on iodine quantification performance. Physics in Medicine and Biology, 2019, 64, 115019.	3.0	18
85	Localization of liver lesions in abdominal CT imaging: II. Mathematical model observer performance correlates with human observer performance for localization of liver lesions in abdominal CT imaging. Physics in Medicine and Biology, 2019, 64, 105012.	3.0	8
86	A deep learning†and partial least square regressionâ€based model observer for a lowâ€contrast lesion detection task in CT. Medical Physics, 2019, 46, 2052-2063.	3.0	27
87	Improving iodine contrast to noise ratio using virtual monoenergetic imaging and prior-knowledge-aware iterative denoising (mono-PKAID). Physics in Medicine and Biology, 2019, 64, 105014.	3.0	19
88	Understanding, justifying, and optimizing radiation exposure for CT imaging in nephrourology. Nature Reviews Urology, 2019, 16, 231-244.	3.8	28
89	Ability of Dual-Energy CT to Detect Silicone Gel Breast Implant Rupture and Nodal Silicone Spread. American Journal of Roentgenology, 2019, 212, 933-942.	2.2	15
90	Individualized Delay for Abdominal Computed Tomography Angiography Bolus-Tracking Based on Sequential Monitoring: Increased Aortic Contrast Permits Decreased Injection Rate and Lower Iodine Dose. Journal of Computer Assisted Tomography, 2019, 43, 612-618.	0.9	8

#	Article	IF	CITATIONS
91	Evaluation of Lower-Dose Spiral Head CT for Detection of Intracranial Findings Causing Neurologic Deficits. American Journal of Neuroradiology, 2019, 40, 1855-1863.	2.4	9
92	High-Resolution Chest Computed Tomography Imaging of the Lungs. Investigative Radiology, 2019, 54, 129-137.	6.2	106
93	Reduction of Metal Artifacts and Improvement in Dose Efficiency Using Photon-Counting Detector Computed Tomography and Tin Filtration. Investigative Radiology, 2019, 54, 204-211.	6.2	76
94	Estimating a sizeâ€specific dose for helical head CT examinations using Monte Carlo simulation methods. Medical Physics, 2019, 46, 902-912.	3.0	10
95	Robustness of Textural Features to Predict Stone Fragility Across Computed Tomography Acquisition and Reconstruction Parameters. Academic Radiology, 2019, 26, 885-892.	2.5	3
96	Findings of CT-Derived Bone Strength Assessment in Inflammatory Bowel Disease Patients Undergoing CT Enterography in Clinical Practice. Inflammatory Bowel Diseases, 2019, 25, 1072-1079.	1.9	11
97	Lead Shielding in Pediatric Chest CT: Effect of Apron Placement Outside the Scan Volume on Radiation Dose Reduction. American Journal of Roentgenology, 2019, 212, 151-156.	2.2	16
98	Impact of Effective Detector Pixel and CT Voxel Size on Accurate Estimation of Blood Volume in Opacified Microvasculature. Academic Radiology, 2019, 26, 1410-1416.	2.5	5
99	Clinical Assessment of Metal Artifact Reduction Methods in Dual-Energy CT Examinations of Instrumented Spines. American Journal of Roentgenology, 2019, 212, 395-401.	2.2	20
100	Breathe New Life Into Your Chest CT Exams: Using Advanced Acquisition and Postprocessing Techniques. Current Problems in Diagnostic Radiology, 2019, 48, 152-160.	1.4	4
101	Impact of prior information on material decomposition in dual- and multienergy computed tomography. Journal of Medical Imaging, 2019, 6, 1.	1.5	7
102	Determination of iodine detectability in different types of multiple-energy images for a photon-counting detector computed tomography system. Journal of Medical Imaging, 2019, 6, 1.	1.5	3
103	Simulation of CT images reconstructed with different kernels using a convolutional neural network and its implications for efficient CT workflow. , 2019, , .		6
104	Correlation between a deep-learning-based model observer and human observer for a realistic lung nodule localization task in chest CT. , 2019, , .		3
105	Multi-contrast imaging on dual-source photon-counting-detector (PCD) CT. , 2019, , .		3
106	Validation of imaging-based quantification of glenohumeral joint kinematics using an unmodified clinical biplane fluoroscopy system. Journal of Biomechanics, 2018, 71, 306-312.	2.1	9
107	Characterization of Urinary Stone Composition by Use of Whole-body, Photon-counting Detector CT. Academic Radiology, 2018, 25, 1270-1276.	2.5	17
108	Targeted Imaging of Renal Fibrosis Using Antibody-Conjugated Gold Nanoparticles in Renal Artery Stenosis. Investigative Radiology, 2018, 53, 623-628.	6.2	15

#	Article	IF	CITATIONS
109	The Changing Incidence and Presentation of Urinary Stones Over 3 Decades. Mayo Clinic Proceedings, 2018, 93, 291-299.	3.0	107
110	Intrarenal fat deposition does not interfere with the measurement of single-kidney perfusion in obese swine using multi-detector computed tomography. Journal of Cardiovascular Computed Tomography, 2018, 12, 149-152.	1.3	9
111	Low kV versus dual-energy virtual monoenergetic CT imaging for proven liver lesions: what are the advantages and trade-offs in conspicuity and image quality? A pilot study. Abdominal Radiology, 2018, 43, 1404-1412.	2.1	30
112	Reproducible imaging features of biologically aggressive gastrointestinal stromal tumors of the small bowel. Abdominal Radiology, 2018, 43, 1567-1574.	2.1	21
113	Concern about a recently published paper in the European Journal of Radiology. European Journal of Radiology, 2018, 109, 203.	2.6	0
114	Comparison of a Photon-Counting-Detector CT with an Energy-Integrating-Detector CT for Temporal Bone Imaging: A Cadaveric Study. American Journal of Neuroradiology, 2018, 39, 1733-1738.	2.4	69
115	Observer Performance with Varying Radiation Dose and Reconstruction Methods for Detection of Hepatic Metastases. Radiology, 2018, 289, 455-464.	7.3	40
116	Theoretical and experimental analysis of photon counting detector CT for proton stopping power prediction. Medical Physics, 2018, 45, 5186-5196.	3.0	11
117	Prospective Pilot Evaluation of Radiologists and Computer-aided Pulmonary Nodule Detection on Ultra–low-Dose CT With Tin Filtration. Journal of Thoracic Imaging, 2018, 33, 396-401.	1.5	21
118	Detection and Characterization of Renal Stones by Using Photon-Counting–based CT. Radiology, 2018, 289, 436-442.	7.3	43
119	Evaluation of projection―and dualâ€energyâ€based methods for metal artifact reduction in <scp>CT</scp> using a phantom study. Journal of Applied Clinical Medical Physics, 2018, 19, 252-260.	1.9	27
120	Material decomposition with prior knowledge aware iterative denoising (MD-PKAID). Physics in Medicine and Biology, 2018, 63, 195003.	3.0	39
121	Estimating lung, breast, and effective dose from lowâ€dose lung cancer screening CT exams with tube current modulation across a range of patient sizes. Medical Physics, 2018, 45, 4667-4682.	3.0	7
122	150-μm Spatial Resolution Using Photon-Counting Detector Computed Tomography Technology. Investigative Radiology, 2018, 53, 655-662.	6.2	137
123	Dual-source multienergy CT with triple or quadruple x-ray beams. Journal of Medical Imaging, 2018, 5, 1.	1.5	14
124	Evaluation of a photon counting Medipix3RX cadmium zinc telluride spectral x-ray detector. Journal of Medical Imaging, 2018, 5, 1.	1.5	4
125	Ultra-high resolution photon-counting detector CT reconstruction using spectral prior image constrained compressed-sensing (UHR-SPICCS). , 2018, 10573, .		7
126	Determination of optimal image type and lowest detectable concentration for iodine detection on a photon counting detector-based multi-energy CT system. , 2018, 10573, .		6

#	Article	IF	CITATIONS
127	Impact of photon counting detector technology on kV selection and diagnostic workflow in CT. , 2018, 10573, .		10
128	Three-material decomposition in multi-energy CT: impact of prior information on noise and bias. , 2018, 10573, .		8
129	Correlation between model observers in uniform background and human observer in patient liver background for a low-contrast detection task in CT. , 2018, 10577, .		2
130	Advocating for use of the <scp>ALARA</scp> principle in the context of medical imaging fails to recognize that the risk is hypothetical and so serves to reinforce patients' fears of radiation. Medical Physics, 2017, 44, 3-6.	3.0	27
131	An effective noise reduction method for multiâ€energy <scp>CT</scp> images that exploit spatioâ€spectral features. Medical Physics, 2017, 44, 1610-1623.	3.0	37
132	Reducing Iodine Contrast Volume in CT Angiography of the Abdominal Aorta Using Integrated Tube Potential Selection and Weight-Based Method Without Compromising Image Quality. American Journal of Roentgenology, 2017, 208, 552-563.	2.2	21
133	Detection of increased vasa vasorum in artery walls: improving CT number accuracy using image deconvolution. , 2017, 10132, .		1
134	Technical Note: Insertion of digital lesions in the projection domain for dualâ€source, dualâ€energy <scp>CT</scp> . Medical Physics, 2017, 44, 1655-1660.	3.0	3
135	Low-Dose CT for Craniosynostosis: Preserving Diagnostic Benefit with Substantial Radiation Dose Reduction. American Journal of Neuroradiology, 2017, 38, 672-677.	2.4	29
136	Selection of optimal tube potential settings for dual-energy CT virtual mono-energetic imaging of iodine in the abdomen. Abdominal Radiology, 2017, 42, 2289-2296.	2.1	14
137	A virtual clinical trial using projection-based nodule insertion to determine radiologist reader performance in lung cancer screening CT. , 2017, 10132, .		6
138	Consistency of Renal Stone Volume Measurements Across CT Scanner Model and Reconstruction Algorithm Configurations. American Journal of Roentgenology, 2017, 209, 116-121.	2.2	5
139	A multi-reader inÂvitro study using porcine kidneys to determine the impact of integrated circuit detectors and iterative reconstruction on the detection accuracy, size measurement, and radiation dose for small (<4 mm) renal stones. Acta Radiologica, 2017, 58, 1012-1019.	1.1	2
140	Estimating patient dose from CT exams that use automatic exposure control: Development and validation of methods to accurately estimate tube current values. Medical Physics, 2017, 44, 4262-4275.	3.0	27
141	Anatomic modeling using 3D printing: quality assurance and optimization. 3D Printing in Medicine, 2017, 3, 6.	3.1	83
142	Correlation between a 2D channelized Hotelling observer and human observers in a lowâ€contrast detection task with multislice reading in <scp>CT</scp> . Medical Physics, 2017, 44, 3990-3999.	3.0	37
143	Evaluation of a projection-domain lung nodule insertion technique in thoracic computed tomography. Journal of Medical Imaging, 2017, 4, 013510.	1.5	4
144	Estimation of Observer Performance for Reduced Radiation Dose Levels in CT. Academic Radiology, 2017, 24, 876-890.	2.5	38

#	Article	IF	CITATIONS
145	Subjective and objective heterogeneity scores for differentiating small renal masses using contrast-enhanced CT. Abdominal Radiology, 2017, 42, 1485-1492.	2.1	34
146	Utility of single-energy and dual-energy computed tomography in clot characterization: An in-vitro study. Interventional Neuroradiology, 2017, 23, 279-284.	1.1	17
147	A comparison of relative proton stopping power measurements across patient size using dual- and single-energy CT. Acta Oncológica, 2017, 56, 1465-1471.	1.8	22
148	Spectral performance of a whole-body research photon counting detector CT: quantitative accuracy in derived image sets. Physics in Medicine and Biology, 2017, 62, 7216-7232.	3.0	90
149	Estimation of signal and noise for a whole-body research photon-counting CT system. Journal of Medical Imaging, 2017, 4, 023505.	1.5	14
150	Practical implementation of channelized hotelling observers: effect of ROI size. Proceedings of SPIE, 2017, 10132, .	0.8	5
151	Lowâ€dose <scp>CT</scp> for the detection and classification of metastatic liver lesions: Results of the 2016 Low Dose <scp>CT</scp> Grand Challenge. Medical Physics, 2017, 44, e339-e352.	3.0	132
152	CT Dental Artifact: Comparison of an Iterative Metal Artifact Reduction Technique with Weighted Filtered Back-Projection. Acta Radiologica Open, 2017, 6, 205846011774327.	0.6	29
153	Use of a channelized Hotelling observer to assess CT image quality and optimize dose reduction for iteratively reconstructed images. Journal of Medical Imaging, 2017, 4, 1.	1.5	9
154	Lung nodule volume quantification and shape differentiation with an ultra-high resolution technique on a photon-counting detector computed tomography system. Journal of Medical Imaging, 2017, 4, 1.	1.5	20
155	Phase-contrast imaging with a compact x-ray light source: system design. Journal of Medical Imaging, 2017, 4, 1.	1.5	1
156	Measuring arterial wall perfusion using photon-counting computed tomography (CT): improving CT number accuracy of artery wall using image deconvolution. Journal of Medical Imaging, 2017, 4, 1.	1.5	7
157	How Low Can We Go in Radiation Dose for the Data-Completion Scan on a Research Whole-Body Photon-Counting Computed Tomography System. Journal of Computer Assisted Tomography, 2016, 40, 663-670.	0.9	47
158	To Scan or not to Scan. Health Physics, 2016, 110, 287-290.	0.5	7
159	An open library of CT patient projection data. Proceedings of SPIE, 2016, 9783, .	0.8	7
160	Dual-source multi-energy CT with triple or quadruple x-ray beams. , 2016, 9783, .		10
161	Estimation of signal and noise for a whole-body photon counting research CT system. Proceedings of SPIE, 2016, 9783, .	0.8	4
162	Arterial wall perfusion measured with photon counting spectral x-ray CT. Proceedings of SPIE, 2016, 9967, .	0.8	12

#	Article	IF	CITATIONS
163	Technical Note: Display window setting: An important factor for detecting subtle but clinically relevant artifacts in daily CT quality control. Medical Physics, 2016, 43, 6413-6417.	3.0	2
164	Technical Note: Improved CT number stability across patient size using dual-energy CT virtual monoenergetic imaging. Medical Physics, 2016, 43, 513-517.	3.0	36
165	Dose-efficient ultrahigh-resolution scan mode using a photon counting detector computed tomography system. Journal of Medical Imaging, 2016, 3, 043504.	1.5	105
166	Noise performance of low-dose CT: comparison between an energy integrating detector and a photon counting detector using a whole-body research photon counting CT scanner. Journal of Medical Imaging, 2016, 3, 043503.	1.5	74
167	Potential Clinical Ramifications of Dose Alert on CT-Guided Interventional Procedures. Journal of the American College of Radiology, 2016, 13, 542-544.	1.8	3
168	The Role of the Medical Physicist in Managing Radiation Dose and Communicating Risk in CT. American Journal of Roentgenology, 2016, 206, 1241-1244.	2.2	13
169	The Role of Dynamic (4D) CT in the Detection of Scapholunate Ligament Injury. Journal of Wrist Surgery, 2016, 05, 306-310.	0.7	33
170	Impact of number of repeated scans on model observer performance for a low-contrast detection task in computed tomography. Journal of Medical Imaging, 2016, 3, 023504.	1.5	15
171	Quantitative Prediction of Stone Fragility From Routine Dual Energy CT. Academic Radiology, 2016, 23, 1545-1552.	2.5	12
172	Spectral prior image constrained compressed sensing (spectral PICCS) for photon-counting computed tomography. Physics in Medicine and Biology, 2016, 61, 6707-6732.	3.0	75
173	Validation of a Projection-domain Insertion of Liver Lesions into CT Images. Academic Radiology, 2016, 23, 1221-1229.	2.5	5
174	Human Imaging With Photon Counting–Based Computed Tomography at Clinical Dose Levels. Investigative Radiology, 2016, 51, 421-429.	6.2	205
175	Evaluation of a projection-domain lung nodule insertion technique in thoracic CT. , 2016, 9783, .		5
176	Construction of realistic phantoms from patient images and a commercial three-dimensional printer. Journal of Medical Imaging, 2016, 3, 033501.	1.5	28
177	Predicting detection performance with model observers: Fourier domain or spatial domain?. Proceedings of SPIE, 2016, 9783, .	0.8	4
178	Evaluation of a photon counting Medipix3RX CZT spectral x-ray detector. Proceedings of SPIE, 2016, 9969, .	0.8	5
179	Dual-Energy CT for Quantification of Urinary Stone Composition in Mixed Stones: A Phantom Study. American Journal of Roentgenology, 2016, 207, 321-329.	2.2	24
180	Dealing with Uncertainty in CT Images. Radiology, 2016, 279, 5-10.	7.3	21

#	Article	IF	CITATIONS
181	Evaluation of conventional imaging performance in a research whole-body CT system with a photon-counting detector array. Physics in Medicine and Biology, 2016, 61, 1572-1595.	3.0	185
182	Relative accuracy of spin-image-based registration of partial capitate bones in 4DCT of the wrist. Computer Methods in Biomechanics and Biomedical Engineering: Imaging and Visualization, 2016, 4, 360-367.	1.9	4
183	The influence of focal spot blooming on highâ€contrast spatial resolution in CT imaging. Medical Physics, 2015, 42, 6011-6020.	3.0	13
184	Technical Note: Development and validation of an open data format for CT projection data. Medical Physics, 2015, 42, 6964-6972.	3.0	25
185	A robust noise reduction technique for time resolved CT. Medical Physics, 2015, 43, 347-359.	3.0	11
186	Lesion insertion in the projection domain: Methods and initial results. Medical Physics, 2015, 42, 7034-7042.	3.0	18
187	Assessment of Low-Contrast Resolution for the American College of Radiology Computed Tomographic Accreditation Program. Journal of Computer Assisted Tomography, 2015, 39, 619-623.	0.9	12
188	The Clinical Impact of Accurate Cystine Calculi Characterization Using Dual-Energy Computed Tomography. Case Reports in Radiology, 2015, 2015, 1-5.	0.3	2
189	Maximizing lodine Contrast-to-Noise Ratios in Abdominal CT Imaging through Use of Energy Domain Noise Reduction and Virtual Monoenergetic Dual-Energy CT. Radiology, 2015, 276, 562-570.	7.3	100
190	Observer Performance in the Detection and Classification of Malignant Hepatic Nodules and Masses with CT Image-Space Denoising and Iterative Reconstruction. Radiology, 2015, 276, 465-478.	7.3	51
191	Image-based material decomposition with a general volume constraint for photon-counting CT. Proceedings of SPIE, 2015, 9412, .	0.8	24
192	Lesion insertion in projection domain for computed tomography image quality assessment. Proceedings of SPIE, 2015, 9412, .	0.8	7
193	Impact of number of repeated scans on model observer performance for a low-contrast detection task in CT. Proceedings of SPIE, 2015, 9416, .	0.8	1
194	Characterization of Urinary Stone Composition by Use of Third-Generation Dual-Source Dual-Energy CT With Increased Spectral Separation. American Journal of Roentgenology, 2015, 205, 1203-1207.	2.2	36
195	Size-specific Dose Estimates for Chest, Abdominal, and Pelvic CT: Effect of Intrapatient Variability in Water-equivalent Diameter. Radiology, 2015, 276, 184-190.	7.3	66
196	Construction of realistic liver phantoms from patient images using 3D printer and its application in CT image quality assessment. , 2015, 2015, .		8
197	Use of Ionizing Radiation in Screening Examinations for Coronary Artery Calcium and Cancers of the Lung, Colon, and Breast. Seminars in Roentgenology, 2015, 50, 148-160.	0.6	4
198	Radiation Dose Reduction in Pediatric Body CT Using Iterative Reconstruction and a Novel Image-Based Denoising Method. American Journal of Roentgenology, 2015, 205, 1026-1037.	2.2	19

#	Article	IF	CITATIONS
199	Dual-energy CT for the diagnosis of gout: an accuracy and diagnostic yield study. Annals of the Rheumatic Diseases, 2015, 74, 1072-1077.	0.9	216
200	Technical Note: Measuring contrast―and noiseâ€dependent spatial resolution of an iterative reconstruction method in CT using ensemble averaging. Medical Physics, 2015, 42, 2261-2267.	3.0	52
201	Answers to Common Questions About the Use and Safety of CT Scans. Mayo Clinic Proceedings, 2015, 90, 1380-1392.	3.0	128
202	Radiation Dose Reduction in Dual-Energy CT: Does It Affect the Accuracy of Urinary Stone Characterization?. American Journal of Roentgenology, 2015, 205, W172-W176.	2.2	14
203	Dual- and Multi-Energy CT: Principles, Technical Approaches, and Clinical Applications. Radiology, 2015, 276, 637-653.	7.3	1,092
204	Degradation of CT Low-Contrast Spatial Resolution Due to the Use of Iterative Reconstruction and Reduced Dose Levels. Radiology, 2015, 276, 499-506.	7.3	116
205	Quantification of Asymptomatic Kidney Stone Burden by Computed Tomography for Predicting Future Symptomatic Stone Events. Urology, 2015, 85, 45-50.	1.0	41
206	Methods for Clinical Evaluation of Noise Reduction Techniques in Abdominopelvic CT. Radiographics, 2014, 34, 849-862.	3.3	123
207	Risks, Benefits, and Risk Reduction Strategies in Thoracic CT Imaging. Seminars in Respiratory and Critical Care Medicine, 2014, 35, 083-090.	2.1	6
208	Automated Assessment of Renal Cortical Surface Roughness From Computerized Tomography Images and Its Association with Age. Academic Radiology, 2014, 21, 1441-1445.	2.5	13
209	Use of CT Dose Notification and Alert Values in Routine Clinical Practice. Journal of the American College of Radiology, 2014, 11, 450-455.	1.8	12
210	Correlation between human and model observer performance for discrimination task in CT. Physics in Medicine and Biology, 2014, 59, 3389-3404.	3.0	41
211	Reducing Image Noise in Computed Tomography (CT) Colonography. Journal of Computer Assisted Tomography, 2014, 38, 398-403.	0.9	18
212	Spatial resolution improvement and dose reduction potential for inner ear CT imaging using a zâ€axis deconvolution technique. Medical Physics, 2013, 40, 061904.	3.0	30
213	Differentiation of Calcium Oxalate Monohydrate and Calcium Oxalate Dihydrate Stones Using Quantitative Morphological Information from Micro-Computerized and Clinical Computerized Tomography. Journal of Urology, 2013, 189, 2350-2356.	0.4	31
214	Prediction of human observer performance in a 2â€alternative forced choice lowâ€contrast detection task using channelized Hotelling observer: Impact of radiation dose and reconstruction algorithms. Medical Physics, 2013, 40, 041908.	3.0	117
215	Adaptive nonlocal means filtering based on local noise level for CT denoising. Medical Physics, 2013, 41, 011908.	3.0	201
216	3D-3D registration of partial capitate bones using spin-images. Proceedings of SPIE, 2013, 8671, .	0.8	2

#	Article	IF	CITATIONS
217	Electronic Noise in CT Detectors: Impact on Image Noise and Artifacts. American Journal of Roentgenology, 2013, 201, W626-W632.	2.2	83
218	Automatic Selection of Tube Potential for Radiation Dose Reduction in Vascular and Contrast-Enhanced Abdominopelvic CT. American Journal of Roentgenology, 2013, 201, W297-W306.	2.2	58
219	Correlation between model observer and human observer performance in CT imaging when lesion location is uncertain. Medical Physics, 2013, 40, 081908.	3.0	83
220	Pilot Study of Detection, Radiologist Confidence and Image Quality With Sinogram-Affirmed Iterative Reconstruction at Half–Routine Dose Level. Journal of Computer Assisted Tomography, 2013, 37, 203-211.	0.9	28
221	Individualized kV Selection and Tube Current Reduction in Excretory Phase Computed Tomography Urography. Journal of Computer Assisted Tomography, 2013, 37, 551-559.	0.9	20
222	Achieving Routine Submillisievert CT Scanning: Report from the Summit on Management of Radiation Dose in CT. Radiology, 2012, 264, 567-580.	7.3	246
223	Noise Reduction to Decrease Radiation Dose and Improve Conspicuity of Hepatic Lesions at Contrast-Enhanced 80-kV Hepatic CT Using Projection Space Denoising. American Journal of Roentgenology, 2012, 198, 405-411.	2.2	37
224	Attenuationâ€based estimation of patient size for the purpose of size specific dose estimation in CT. Part II. Implementation on abdomen and thorax phantoms using cross sectional CT images and scanned projection radiograph images. Medical Physics, 2012, 39, 6772-6778.	3.0	67
225	Attenuationâ€based estimation of patient size for the purpose of size specific dose estimation in CT. Part I. Development and validation of methods using the CT image. Medical Physics, 2012, 39, 6764-6771.	3.0	76
226	Toward Biphasic Computed Tomography (CT) Enteric Contrast. Journal of Computer Assisted Tomography, 2012, 36, 554-559.	0.9	26
227	Development and Validation of a Practical Lower-Dose-Simulation Tool for Optimizing Computed Tomography Scan Protocols. Journal of Computer Assisted Tomography, 2012, 36, 477-487.	0.9	119
228	Applications of Dual-Energy CT in Urologic Imaging: An Update. Radiologic Clinics of North America, 2012, 50, 191-205.	1.8	53
229	Dual-Energy CT–Based Monochromatic Imaging. American Journal of Roentgenology, 2012, 199, S9-S15.	2.2	483
230	Kidney Stone Volume Estimation from Computerized Tomography Images Using a Model Based Method of Correcting for the Point Spread Function. Journal of Urology, 2012, 188, 989-995.	0.4	19
231	The use of bismuth breast shields for CT should be discouraged. Medical Physics, 2012, 39, 2321-2324.	3.0	27
232	CT Dose Index and Patient Dose: They Are <i>Not</i> the Same Thing. Radiology, 2011, 259, 311-316.	7.3	377
233	Bismuth Shields for CT Dose Reduction: Do They Help or Hurt?. Journal of the American College of Radiology, 2011, 8, 878-879.	1.8	14
234	Noise reduction in spectral CT: Reducing dose and breaking the tradeâ€off between image noise and energy bin selection. Medical Physics, 2011, 38, 4946-4957.	3.0	95

#	Article	IF	CITATIONS
235	Identification of Intraarticular and Periarticular Uric Acid Crystals with Dual-Energy CT: Initial Evaluation. Radiology, 2011, 261, 516-524.	7.3	211
236	Optimal Tube Potential for Radiation Dose Reduction in Pediatric CT: Principles, Clinical Implementations, and Pitfalls. Radiographics, 2011, 31, 835-848.	3.3	179
237	Prospective Blinded Comparison of Wireless Capsule Endoscopy and Multiphase CT Enterography in Obscure Gastrointestinal Bleeding. Radiology, 2011, 260, 744-751.	7.3	150
238	Virtual monochromatic imaging in dualâ€source dualâ€energy CT: Radiation dose and image quality. Medical Physics, 2011, 38, 6371-6379.	3.0	282
239	Dual-Energy Dual-Source CT With Additional Spectral Filtration Can Improve the Differentiation of Non–Uric Acid Renal Stones: An Ex Vivo Phantom Study. American Journal of Roentgenology, 2011, 196, 1279-1287.	2.2	120
240	Automatic selection of tube potential for radiation dose reduction in CT: A general strategy. Medical Physics, 2010, 37, 234-243.	3.0	201
241	Appropriate Patient Selection at Abdominal Dual-Energy CT Using 80 kV: Relationship between Patient Size, Image Noise, and Image Quality. Radiology, 2010, 257, 732-742.	7.3	136
242	How Effective Is Effective Dose as a Predictor of Radiation Risk?. American Journal of Roentgenology, 2010, 194, 890-896.	2.2	137
243	Dual-Source Dual-Energy CT With Additional Tin Filtration: Dose and Image Quality Evaluation in Phantoms and In Vivo. American Journal of Roentgenology, 2010, 195, 1164-1174.	2.2	170
244	Imaging evaluation and treatment of nephrolithiasis: an update. Minnesota Medicine, 2010, 93, 48-51.	0.1	1
245	Renal Perfusion and Hemodynamics: Accurate in Vivo Determination at CT with a 10-Fold Decrease in Radiation Dose and HYPR Noise Reduction. Radiology, 2009, 253, 98-105.	7.3	36
246	In Defense of Body CT. American Journal of Roentgenology, 2009, 193, 28-39.	2.2	144
247	Image quality optimization and evaluation of linearly mixed images in dualâ€source, dualâ€energy CT. Medical Physics, 2009, 36, 1019-1024.	3.0	147
248	Quantitative imaging of element composition and mass fraction using dualâ€energy CT: Threeâ€material decomposition. Medical Physics, 2009, 36, 1602-1609.	3.0	253
249	Radiation dose reduction in computed tomography: techniques and future perspective. Imaging in Medicine, 2009, 1, 65-84.	0.0	296
250	Dualâ€source spiral CT with pitch up to 3.2 and 75 ms temporal resolution: Image reconstruction and assessment of image quality. Medical Physics, 2009, 36, 5641-5653.	3.0	155
251	Strategies for Reducing Radiation Dose in CT. Radiologic Clinics of North America, 2009, 47, 27-40.	1.8	650
252	Measurement of temporal resolution in dual source CT. Medical Physics, 2008, 35, 764-768.	3.0	34

#	Article	IF	CITATIONS
253	Radiation Exposure and Pregnancy: When Should We Be Concerned?. Radiographics, 2007, 27, 909-917.	3.3	464
254	Assessment of Renal Hemodynamics and Function in Pigs with 64-Section Multidetector CT: Comparison with Electron-Beam CT. Radiology, 2007, 243, 405-412.	7.3	109
255	Effects of CT Irradiation on Implantable Cardiac Rhythm Management Devices1. Radiology, 2007, 243, 766-774.	7.3	61
256	Coronary Artery Calcium: A Multi-institutional, Multimanufacturer International Standard for Quantification at Cardiac CT. Radiology, 2007, 243, 527-538.	7.3	256
257	Evaluation of Porcine Myocardial Microvascular Permeability and Fractional Vascular Volume Using 64-Slice Helical Computed Tomography (CT). Investigative Radiology, 2007, 42, 274-282.	6.2	37
258	Dose Performance of a 64-Channel Dual-Source CT Scanner1. Radiology, 2007, 243, 775-784.	7.3	192
259	Noninvasive Differentiation of Uric Acid versus Non–Uric Acid Kidney Stones Using Dual-Energy CT. Academic Radiology, 2007, 14, 1441-1447.	2.5	364
260	First performance evaluation of a dual-source CT (DSCT) system. European Radiology, 2006, 16, 256-268.	4.5	1,296
261	Relationship between Noise, Dose, and Pitch in Cardiac Multi–Detector Row CT. Radiographics, 2006, 26, 1785-1794.	3.3	159
262	CT Dose Reduction and Dose Management Tools: Overview of Available Options. Radiographics, 2006, 26, 503-512.	3.3	704
263	Automatic Exposure Control in CT: Are We Done Yet?. Radiology, 2005, 237, 755-756.	7.3	53
264	The phantom portion of the American College of Radiology (ACR) Computed Tomography (CT) accreditation program: Practical tips, artifact examples, and pitfalls to avoid. Medical Physics, 2004, 31, 2423-2442.	3.0	138
265	Patient Dose in Cardiac Computed Tomography. Herz, 2003, 28, 1-6.	1.1	90
266	Measurement of half-value layer in x-ray CT: A comparison of two noninvasive techniques. Medical Physics, 2000, 27, 1915-1919.	3.0	47
267	Calculation of effective dose. Medical Physics, 2000, 27, 828-837.	3.0	236
268	Experimental determination of section sensitivity profiles and image noise in electron beam computed tomography. Medical Physics, 1999, 26, 287-295.	3.0	9
269	Performance evaluation of a multi-slice CT system. Medical Physics, 1999, 26, 2223-2230.	3.0	348
270	The measurement of radiation dose profiles for electron-beam computed tomography using film dosimetry. Medical Physics, 1994, 21, 1287-1291.	3.0	8

#	Article	IF	CITATIONS
271	Medical Imaging Physics , by W. R. Hendee and E. R. Ritenour. Medical Physics, 1994, 21, 328-329.	3.0	о